

VIRGi: View-dependent Instant Recoloring of 3D Gaussians Splats

Alessio Mazzucchelli, Ivan Ojeda-Martin, Fernando Rivas-Manzaneque, Elena Garces, Adrian Penate-Sanchez, Francesc Moreno-Noguer

Abstract—3D Gaussian Splatting (3DGS) has recently transformed the fields of novel view synthesis and 3D reconstruction due to its ability to accurately model complex 3D scenes and its unprecedented rendering performance. However, a significant challenge persists: the absence of an efficient and photorealistic method for editing the appearance of the scene’s content. In this paper we introduce **VIRGi**, a novel approach for rapidly editing the color of scenes modeled by 3DGS while preserving view-dependent effects such as specular highlights. Key to our method are a novel architecture that separates color into diffuse and view-dependent components, and a multi-view training strategy that integrates image patches from multiple viewpoints. Improving over the conventional single-view batch training, our 3DGS representation provides more accurate reconstruction and serves as a solid representation for the recoloring task. For 3DGS recoloring, we then introduce a rapid scheme requiring only one manually edited image of the scene from the end-user. By fine-tuning the weights of a single MLP, alongside a module for single-shot segmentation of the editable area, the color edits are seamlessly propagated to the entire scene in just two seconds, facilitating real-time interaction and providing control over the strength of the view-dependent effects. An exhaustive validation on diverse datasets demonstrates significant quantitative and qualitative advancements over competitors based on Neural Radiance Fields representations.

Index Terms—Neural Radiance Fields, 3D Gaussian Splatting, Recoloring, Editing, Multi-view Consistency

I. INTRODUCTION

3D Gaussian Splatting (3DGS) [1] has recently established itself as a dominant technique in the fields of 3D reconstruction and image-based rendering. By employing a large set of anisotropic Gaussians to represent scenes, 3DGS facilitates rapid reconstruction and rendering processes, effectively preserving fine details and complex lighting effects. Compared to previous neural rendering methodologies such as NeRFs [2], 3DGS demonstrates markedly superior efficiency

in both reconstruction and rendering. 3DGS has application in various downstream tasks, including 3D scene/object manipulation [3]–[5], instruction-based editing [6], [7], drag-based editing [8], multi-object interaction [9] and style transfer [10], [11]. However, unlike NeRFs, which has been extensively studied for its recoloring capabilities [12]–[16], the recoloring problem has received little attention in the context of 3DGS. In this paper we introduce **VIRGi**, the first approach for photorealistic appearance editing of scenes modeled with 3DGS. Our approach is highly efficient and user friendly. Given a scene modeled with 3DGS, the user simply provides color edits in a single view. These edits are then rapidly propagated throughout the entire scene and viewpoints within approximately two seconds. This, combined with the inherent rendering efficiency of 3DGS, enables a quasi-real-time interactive editing experience.

Our solution is built upon two primary components. First, we present a novel architecture and training scheme tailored for accurately modeling viewpoint dependencies. Traditional 3DGS systems [1] are trained on a per-view basis, with training batches composed of image tiles from a single viewpoint. In our approach we implement multi-view training by modifying the CUDA implementation of the rasterizer, enabling the use of different viewpoints in the same training batch. This approach, as we will show later, facilitates the decomposition of reflections into diffuse and view-dependent components (e.g. specularities), encapsulated in two independent MLPs. The second component of our approach is a pipeline for efficient scene recoloring. Given a target view with the desired color edition, we propose a strategy where we only fine-tune the last layer of the diffuse MLP, in conjunction with a module designed to perform soft segmentation of the edited region. This optimization ensures the consistent propagation of color edits throughout the entire scene, preserving view-dependent effects and preventing artifacts such as color bleeding commonly observed in other approaches. Since this process operates at interactive rates, users can recursively provide new edited images if required. We validate our recoloring method across multiple datasets and conduct a comparative analysis with previous NeRF-based methodologies. **VIRGi** consistently outperforms these approaches not only in efficiency and interactivity but also in quality. We demonstrate that our decoupled diffuse/view-dependent color modeling enables the creation of highly photorealistic color editions, while also empowering the user to control specular effects, such as the strength of the highlights. Fig. 1, and the supplementary video showcase examples of the results achieved with our method, consistently

A. Mazzucchelli is with Arquimea Research Center, San Cristóbal de la Laguna, Santa Cruz de Tenerife, 38320 and Universidad Politécnica de Catalunya, Doctoral Degree in Automatic Control, Robotics and Vision, Carrer de Jordi Girona, 31, Les Corts, Barcelona, 08034, Spain.

I. Ojeda-Martin is with Arquimea Research Center, San Cristóbal de la Laguna, Santa Cruz de Tenerife, 38320.

F. Rivas-Manzaneque is with Volinga AI, San Cristóbal de la Laguna, Santa Cruz de Tenerife, 38320 and Universidad Politécnica de Madrid, Programa de Doctorado en Automática y Robótica, Calle de José Gutiérrez Abascal 2, Madrid, 28006, Spain.

E. Garces is with Universidad Rey Juan Carlos, C/Tulipán S/N, 28933 Móstoles (Madrid), Spain

A. Penate-Sanchez is with IUSANI, Universidad de Las Palmas de Gran Canaria, C/ Juan de Quesada 30, Las Palmas de Gran Canaria, 35001, Spain.

F. Moreno-Noguer is with Institut de Robòtica i Informàtica Industrial (IRI), CSIC-UPC, C/ Llorens i Artigas 4, Barcelona, 08028, Spain.

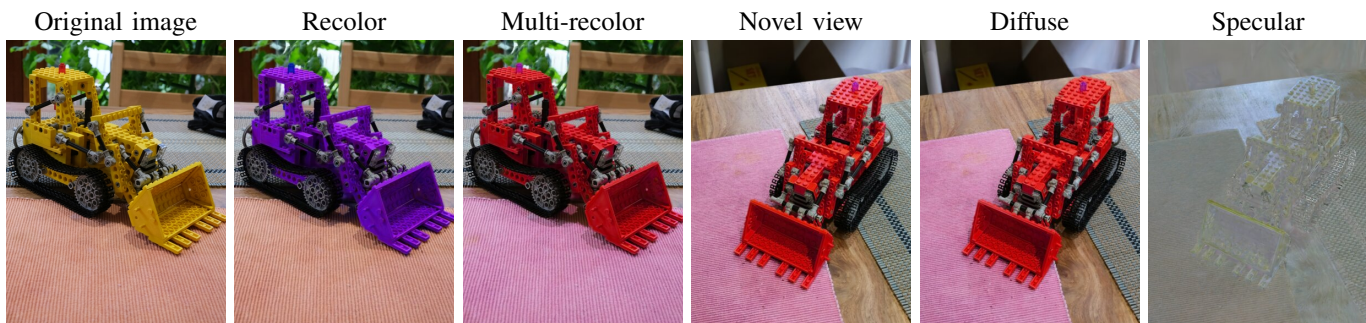


Fig. 1: **VIRGi** enables – by editing a single view – instant recolorings of one or multiple objects in scenes modeled with 3D Gaussian Splats. Our key idea of decomposing the reflectance of the scene into diffuse and specular components allows view-dependent consistent edits. Our separation can also be used to enhance or reduce material specularity.

surpassing competing approaches as demonstrated in Fig. 2. To summarize, we provide the following contributions:

- The first method for conducting photorealistic, view-dependent, and interactive color edits for scenes modeled with Gaussian Splats. Our approach is designed to be user-friendly and interactive, requiring only a single color edit from one view to recolor the entire scene.
- A novel neural network architecture for 3DGS that learns the decoupling of color into its specular and diffuse components. This architecture enables precise color editing of scenes while preserving their view-dependent effects.
- A multi-view training strategy that is essential to learning the diffuse/specular color components. Incorporating information from different viewpoints during training enhances not only the learning of the decomposed output in our novel architecture, but also the overall performance of the 3DGS reconstruction.

II. RELATED WORK

3D Gaussian Splatting [1] provides real-time rendering with simpler manipulation compared to Neural Radiance Fields (NeRFs) [2] because of its explicit scene representation. However, globally editing 3DGS scenes remains an open problem, as we discuss in this section.

Point and 3DGS Rendering. Gaussian Splats originate from point-cloud representations [17]. These techniques became very popular in 3D modeling [18], [19] and as the basis for image-based rendering techniques [20]–[24]. In recent years, Gaussian Splats [1] have surpassed previous point-based rendering methods by enabling real-time novel view synthesis for scenes of varying complexity. These scenes range from those with simple Lambertian materials to those with intricate light interactions, dynamic elements [9], [25]–[30], physical simulators [9], and avatars [31]–[39].

Many works have already addressed the memory and storage limitations of 3DGS, leading to efficient compression strategies that now allow deployment even on lightweight devices [40]. In particular, vector clustering and quantization-based methods have proven effective in minimizing parameter counts [41]–[44]. Notably, [45] employ vector quantization to construct codebooks. However, unlike other methods, their approach explicitly separates color information from geometry.

A major drawback that remains to be addressed, and which we tackle in this paper, is the constraint of performing the optimization step over a single image. Unlike NeRF, where rays from different viewpoints can be sampled with minimal overhead, the 3DGS rasterization pipeline is inherently built around a single image. In this work, we adopt the representation from [45] and extend it by augmenting the CUDA rasterizer so that optimization can be done from multiple images in a single step.

Inverse Rendering in Radiance Fields. NeRF-based approaches have incorporated surface normals and separated diffuse/specular components to improve reflectance modeling and enable scene relighting, as demonstrated in [46], [47]. Other works [48]–[50] jointly optimize geometry, materials, and illumination, leveraging physics-based priors or path tracing with near-field indirect light to better disentangle reflective properties from environmental lighting. In the domain of 3D Gaussian Splatting, inverse rendering has been enhanced by estimating normals, materials, and indirect lighting for each Gaussian primitive [51]. To better handle ambiguities between surface normals and roughness, a segmentation prior is introduced in [52], guiding geometry and material decomposition. Normals are estimated from the shape of each Gaussian in [53], where directional masking enforces orientation, enabling BRDF rendering and disentangling indirect light via voxel-based tracing. A dedicated specular shading is proposed in [54] to refine surface normals and enhance high-frequency reflections without compromising splatting efficiency.

Color Editing. Color editing through edit propagation strategies utilizes local color cues, such as user-defined scribbles or points, to influence similar regions within the image. Previous works in this domain employed propagation rules based on color similarity metrics [55]–[58]. However, defining effective metrics that capture both local and non-local image features posed a challenge. To address this, Convolutional Neural Networks (CNNs) proved successful for robust feature extraction [59], [60]. A different approach involves pre-computed palettes representing dominant colors in an image. These palettes serve as a basis for describing other colors through linear combinations. Some artists prefer this method for its control over global and local color modifications, often combining it with object segmentation techniques [61]–[63].

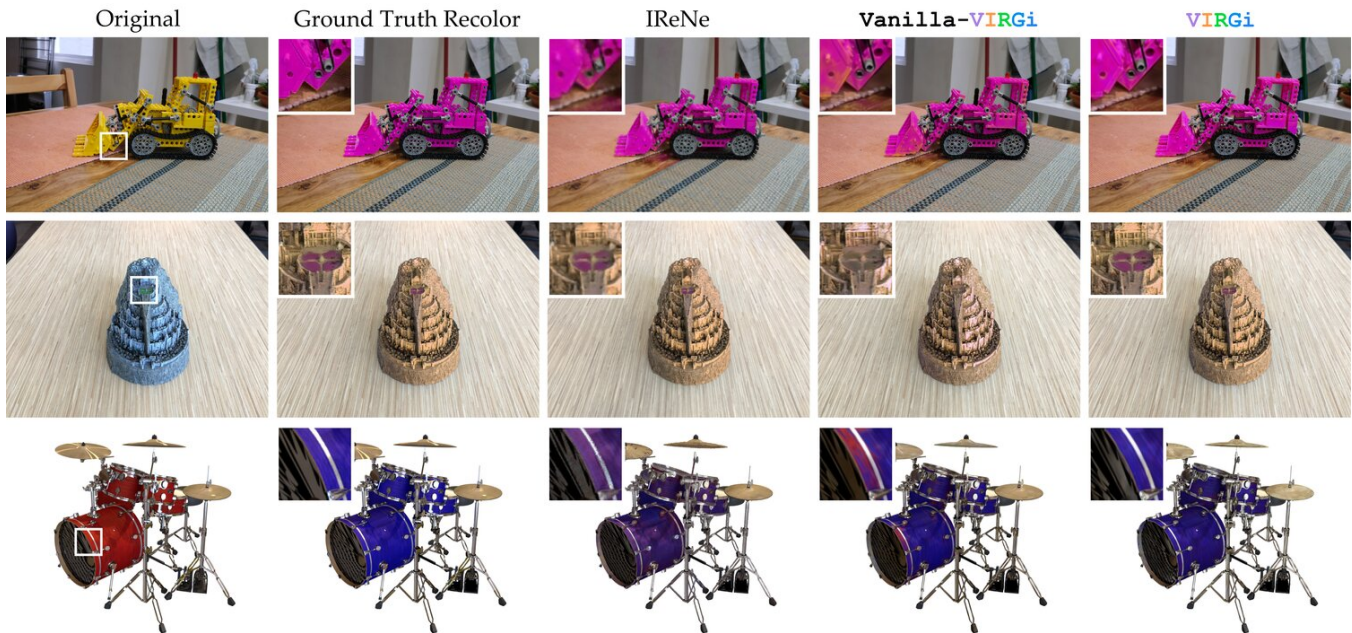


Fig. 2: **Comparison of recoloring methods with a ground truth recolor.** Our method **VIRGi** is the first one to propose a solution for 3DGS recoloring, outperforming one of the best methods in NeRFs recoloring [15] (IReNe). We propose several contributions that make our method robust and better than a baseline (VANILLA-VIRGi) obtained by naïvely combining existing methods.

In this work, we propose a method that can leverage any of these paradigms to transition from a 2D to a full 3D edit. Our method allows users to edit a single 2D image using their preferred editing tool or technique. Thanks to our efficient propagation strategy, any 2D recoloring is extrapolated to a 3DGS-based representation.

Radiance Fields Color Editing. Despite their brief existence, Gaussian Splats have sparked rapid development, with various manipulation techniques emerging. Text prompts are used to modify static scenes [6], [64], [65] or dynamic ones [66], [67]. Additionally, [68] enable object selection, while [69] create articulated Gaussian Splats from dynamic sequences. [5] propose diverse edits, such as semantic segmentation, object segmentation, or text-based editing, through feature distillation. Unlike for NeRFs [12]–[14], [16], to the best of our knowledge, there is no specific work for Gaussian Splat recoloring. Our work draws inspiration from [15], who, by fine-tuning part of the NeRF, achieved remarkable quality and view-dependent instant recoloring. However, as we will demonstrate in the experimental section, our method, which incorporates multi-view training and explicit diffuse/specular modeling, significantly enhances the quality compared to [15].

III. BACKGROUND AND VANILLA-VIRGi

We ground our approach on 3D Gaussian Splatting (3DGS) [1], particularly focusing on Compact 3D Gaussian Splatting (C3DGS) [45]. 3DGS represents the radiance field by generating a collection of 3D Gaussians, each incorporating spherical harmonics information. During the rendering process, these Gaussians are splatted onto a 2D plane to produce the 2D image [70]. However, a notable limitation of 3DGS is

its significant memory requirement, averaging 746 MB for the Mip-NeRF dataset [71]. To address this challenge, C3DGS introduced two solutions: encoding the Gaussians using a codebook to conserve memory, and a key contribution for our purposes, utilizing a hashgrid and an MLP to encode appearance information. Their latter contribution eliminates the necessity to store spherical harmonics coefficients for each Gaussian, thereby reducing the memory footprint by a factor of 15. Consequently, the memory requirements decrease substantially to an average of 48.8 MB on Mip-NeRF dataset. Our proposed approach adapts the recoloring strategy for NeRFs from IReNe [15], one of the top-performing methods in this domain. IReNe takes as input a single recolored view of the NeRF and propagates the edits to the entire NeRF using a strategy based on fine-tuning part of the color MLPs, selecting the neurons responsible for view-dependent effects, and performing soft segmentation in 3D space. We leverage some of these concepts and tailor them to suit C3DGS.

A. VANILLA-VIRGi

Given the differing radiance field representations between NeRFs and 3DGS, combining both strategies presents challenges. Our initial idea, dubbed VANILLA-VIRGi, attempted to integrate the MLP configuration and hashgrid features from C3DGS, along with the last layer and soft-segmentation blending from IReNe in a straightforward manner. Specifically, VANILLA-VIRGi utilizes a single neural network to estimate the color C of each Gaussian, following the formulation proposed in [45], expressed as:

$$C = \text{MLP}_c(f, \theta | \phi_c), \quad (1)$$

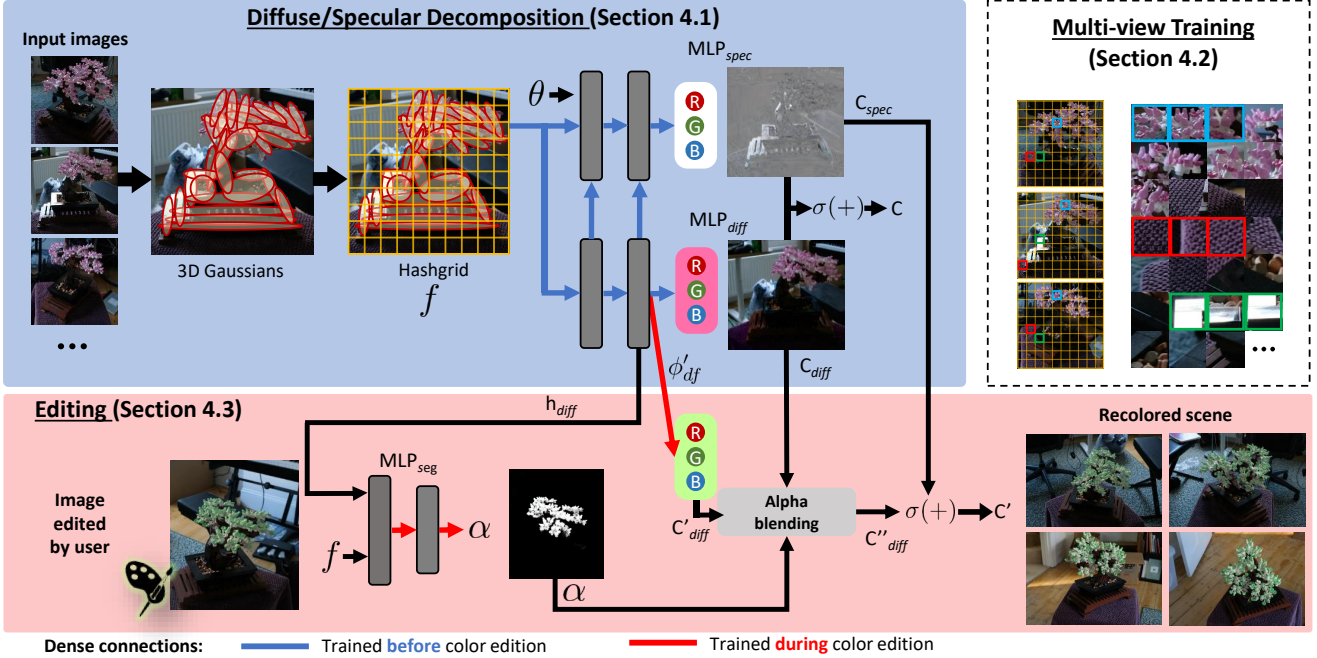


Fig. 3: **Overview of VIRGi.** Our method comprises two main steps. In the initial step, we train a 3DGS architecture consisting of a Hashgrid f representing the geometry and two MLPs for color modeling. We separate the observed color into a diffuse term MLP_{diff} , which solely relies on hashgrid features f , and a specular term MLP_{spec} , which incorporates the view direction θ . Our training strategy involves leveraging multiple views of the same scene point in a single batch, as opposed to using a single image per batch, resulting in improved PSNR compared to previous methods. In the second step, given an edited 2D image, we fine-tune the last layer of the diffuse MLP using a soft-segmentation mask α to achieve the target color.

where f are the hashgrid features, θ denotes the view direction, and ϕ_c are the weights of the MLP. Then, following the approach outlined in IReNe [15], VANILLA-VIRGi modifies only the last layer of MLP_c when an edit is performed, resulting in a new color:

$$C' = \text{MLP}_c(f, \theta | \phi_c^{\text{last}}). \quad (2)$$

C' is blended with the original to produce the final color C'' :

$$C'' = \alpha C' + (1 - \alpha)C. \quad (3)$$

Blending is performed as $\alpha = \text{MLP}_{\text{seg}}(f)$, which is a soft segmentation of the edited region and is learned by an MLP from the hashgrid space features. Additionally, this approach incorporates a view-dependent neuron selection strategy within the last layer of MLP_c . For further details, we encourage readers to refer to the original paper [15].

However, as depicted in Figure 2, this straightforward approach does not yield optimal results, as traces of the previous color persist in the rendering of novel views. This outcome is somewhat expected, as this method lacks mechanisms to enforce multi-view consistency, leading to the entanglement of view-dependent effects such as specular highlights within the color MLP_c .

Our proposed solution, VIRGi, aims to establish a clear separation between diffuse and view-dependent (specular) effects [13], [72], [73] from the initial construction of the Gaussian Splats. We introduce two pivotal concepts detailed in the following section: Firstly, a decoupled diffuse-specular

color estimation through distinct MLPs; and secondly, a multi-view training strategy that leverages the principle that the diffuse color of an object with isotropic reflectance remains invariant to view changes [74].

IV. METHOD

Figure 3 provides an overview of our method, which operates in two main steps. First, we initiate the process by constructing a compact 3D scene representation [45] from a collection of multi-view images. This learned representation comprises two primary components: (i) a set of hashgrid features f , which capture the geometric details of the scene, and (ii) a pair of Multi-Layer Perceptrons (MLPs) responsible for encoding the scene’s appearance. Unlike C3DGS, we employ separate MLPs, MLP_{diff} and MLP_{spec} , to model diffuse color C_{diff} and specular C_{spec} reflections, respectively. The architecture of this decoupling is explained in Section IV-A.

To train our 3DGS, we employ a novel optimized multi-view training strategy, detailed in Section IV-B, that implicitly encourages corresponding 3D points to occupy nearby locations within the neural feature space. This novel approach, unlike conventional training with single images per batch [1], [45], captures more consistent and better reflections, as demonstrated in the experiments section. Once the original scene is learned, users can utilize any existing tool to recolor one view of the scene I^{edit} . Subsequently, our optimized fine-tuning process, described in Section IV-C, ensures that the color edits are consistently propagated throughout the entire scene at interactive rates.

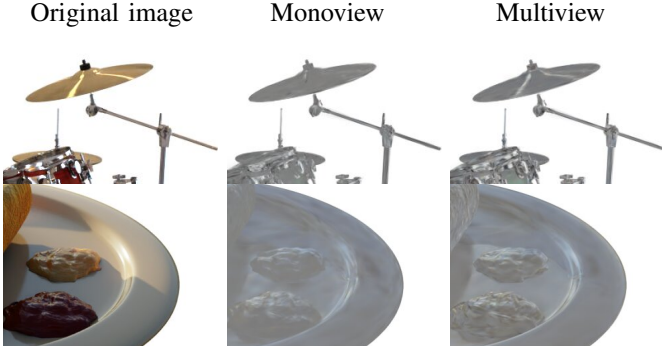


Fig. 4: **Specularity Comparison: Monoview vs. Multiview.** Training with a single viewpoint poses challenges in learning specularities due to limited sample diversity, multiview training facilitates an easier understanding of specular effects.

A. Diffuse/Specular Decomposition Architecture

Separating diffuse C_{diff} and view-dependent color C_{spec} (or specular) in independent MLPs [13], [15] is essential for ensuring view-dependent consistency in the edits. This separation reflects the underlying assumption that object color is primarily captured by the diffuse component which is reasonable for many common scenarios.

To model the view dependency, MLP_{diff} only utilizes the hashgrid features f , whereas MLP_{spec} incorporates both the hashgrid features and the view direction θ . The outputs of these components are combined using a sigmoid function $\sigma(\cdot)$, expressed formally as:

$$C_{\text{diff}} = \text{MLP}_{\text{diff}}(f | \phi_{df}) \quad (4)$$

$$C_{\text{spec}} = \text{MLP}_{\text{spec}}(f, \theta | \phi_{sp}, \phi_{df}) \quad (5)$$

$$C = \sigma(C_{\text{diff}} + C_{\text{spec}}) \quad (6)$$

where ϕ_{sp} and ϕ_{df} denote the specular and diffuse weights of the MLPs, respectively, and C represents the RGB color of the Gaussian.

The standard architecture of MLP_{spec} and MLP_{diff} consists of three fully-connected layers. However, we found it necessary to introduce additional residual connections between them. Specifically, we connected the first layer of MLP_{diff} to the second layer of MLP_{spec} , and the second layer of MLP_{diff} to the third layer of MLP_{spec} . These connections are unidirectional, allowing only MLP_{spec} to access the content of MLP_{diff} .

The rationale behind this architecture is as follows: while MLP_{spec} theoretically accounts for all view-dependent reflectance (since it receives θ as input), MLP_{diff} should focus solely on learning what is view-point invariant. Without these connections, the specular component tends to be noisier, making it challenging to learn an accurate reflection. With the added connections, the specular component gains a better understanding of which aspects of the reflection to prioritize. To train the pair of MLPs we use the following loss function:

$$\mathcal{L} = \|C - I^{\text{edit}}\|_1 + \lambda_{\text{spec}} \|C_{\text{spec}}\|_2^2 \quad (7)$$

This loss function uses an L_1 photometric loss with a smoothness term on the specular component. The value of λ_{spec} gradually decreases from 0.25 to 0.05 during training. Initially, this penalty encourages the network to prioritize explaining color

variations using the diffuse component (C_{diff}) alone. Since the diffuse MLP (MLP_{diff}) lacks view direction information, it cannot effectively capture view-dependent effects. As training progresses, we reduce the penalty on MLP_{spec} to allow the network to also account for the view-dependent part.

B. Multi-view Training

An essential aspect of our method is the multi-view training strategy. Unlike existing approaches in Gaussian Splats [1], [45], which utilize one image per batch, our method samples multiple views simultaneously. This strategy offers two key advantages. Firstly, it encourages points in the 3D world with similar reflectance properties to be close together in the feature space, thereby aiding convergence and enhancing overall quality. Secondly, it assists in implicitly decomposing the reflection into diffuse and specular components, which proves advantageous for the recoloring task.

We adapted the CUDA implementation of the fast rasterizer to use tiles from different images within the same training step. Additionally, to expedite training time without altering the geometry during recoloring, we initialize the 3D Gaussians using C3DGS and freeze them. This ensures interactivity, enabling faster operations as there’s no need to recompute the gaussian ordering for alpha blending during rasterization. With the precomputed ordering, we create mini-batches composed of five tiles from different images, where the same gaussian is observed from diverse viewpoints. The training batch is comprised of as many 5-sample mini-batches as can be accommodated within the GPU’s VRAM.

As we demonstrate in the experimental section, this modification alone significantly enhances the default rendering quality of different baselines (see Table III). Additionally, multi-view training is essential for effectively learning a robust decomposition of both diffuse and view-dependent components. In the original 3DGS approach, training is conducted using a single image per batch, meaning each Gaussian is updated based on this singular viewpoint. However, by including five samples of each Gaussian within the same training batch, the update process endeavors to account for all these viewpoints simultaneously. This aids the MLP_{diff} in discerning the shared color aspects (diffuse) and the viewpoint-dependent characteristics (specular) among these five tiles. In Fig. 4, we provide two examples where the benefits of utilizing multi-view training for learning the specular components are evident.

C. Editing

The recoloring process involves the user modifying a designated target view I^{edit} , followed by fine-tuning a portion of the architecture to accommodate the desired changes. Drawing from [15], we implement last-layer adaptation on the diffuse component (as per Equation 2) and soft-segmentation (as per Equation 3). We update the weights ϕ_{df} of the last layer of MLP_{diff} to derive a new diffuse color C'_{diff} . This new color is then alpha-blended with C_{diff} using the soft-segmentation mask, denoted as α , resulting in the final diffuse color denoted C''_{diff} . It’s worth noting that our method differs in the way the soft-segmentation mask is obtained compared to [15]. In our approach, we establish a connection between the

Method	Mip NeRF 360 [71]			LLFF [75]			NeRF Synthetic [2]		
	PSNR↑	SSIM↑	LPIPS↓	PSNR↑	SSIM↑	LPIPS↓	PSNR↑	SSIM↑	LPIPS↓
PaletteNeRF	22.24	0.720	0.278	24.19	0.800	0.187	29.92	0.960	0.038
RecolorNeRF	-	-	-	24.52	0.736	0.333	29.00	0.943	0.048
IReNe	26.80	0.714	0.292	26.51	0.823	0.136	30.33	0.959	0.035
VANILLA-VIRGi	<u>29.19</u>	<u>0.881</u>	<u>0.150</u>	<u>28.01</u>	<u>0.905</u>	<u>0.129</u>	32.13	0.975	0.023
VIRGi	29.74	0.886	0.146	29.10	0.915	0.119	<u>31.65</u>	<u>0.971</u>	<u>0.027</u>

TABLE I: **Quantitative color edition results. Best, Second.** Results using the recolored ground truth images from [15].

DC	MV	DS	Mip NeRF 360	LLFF	NeRF Synthetic
			PSNR↑	PSNR↑	PSNR↑
\times	\times	\times	29.19	28.01	32.13
\times	\checkmark	\times	29.45	28.54	<u>31.90</u>
\times	\checkmark	\checkmark	29.56	28.62	31.78
\checkmark	\times	\times	28.58	27.66	30.93
\checkmark	\checkmark	\times	<u>29.61</u>	29.15	31.50
\checkmark	\checkmark	\checkmark	29.74	<u>29.10</u>	31.65

TABLE II: **Ablation study. Recoloring results on all datasets of our ablated method. Best, Second.** DC indicates if the output is decoupled or not. MV indicates if the model has been trained using our multi-view rasterization DS indicates if the diffuse’s network MLP_{diff} output has been introduced into the soft segmentation network MLP_{seg}.

activations of last layer of the diffuse MLP, denoted as h_{diff} , and the segmentation MLP. This integration aims to introduce additional contextual information to improve the quality of segmentation. As demonstrated in the experiments section, this enhancement contributes to the overall performance of our approach.

$$\alpha = \text{MLP}_{\text{seg}}(f, h_{\text{diff}}), \quad (8)$$

$$C'_{\text{diff}} = \text{MLP}_{\text{diff}}(f | \phi'_{df}), \quad (9)$$

$$C''_{\text{diff}} = \alpha C'_{\text{diff}} + (1 - \alpha) C_{\text{diff}}, \quad (10)$$

$$C' = \sigma(C''_{\text{diff}} + C_{\text{spec}}) \quad (11)$$

Upon receiving the user’s edit, we fine-tune the color and segmentation MLPs (MLP_{diff}, MLP_{spec}, and MLP_{seg}) to accommodate the desired changes with the following loss function:

$$\mathcal{L} = \|C' - I^{\text{edit}}\|_1 \quad (12)$$

This loss function uses an L_1 photometric loss between the rendered recolored version C' and the user’s edit I^{edit} .

V. RESULTS

A. Quantitative results

Comparison with state-of-the-art. In Table I, we present the results of recoloring on the dataset provided by [15], which includes manually recolored scenes using photoshop in LLFF [75], MipNeRF-360 [71], and recolored scenes from Synthetic NeRF [2] using Blender. The original code from [1] did not converge in the flower and leafs scenes from LLFF, so those scenes were not evaluated for any of the reported methods. We compare our results against several recent baselines, including PaletteNeRF [13], RecolorNeRF [12], and IReNe [15]. We provide results from our proposed method, VIRGi, as well as from the VANILLA-VIRGi. In Fig. 8 some qualitative results from the dataset can be seen. The evaluation

Dataset (PSNR↑)	Mip NeRF 360	LLFF	NeRF Synthetic
Mono-view C3DGS	28.96	25.63	35.60
Multi-view C3DGS	29.47	25.87	35.84
Mono-view VIRGi	28.43	25.73	33.87
Multi-view VIRGi	29.30	25.97	35.76

TABLE III: **Multi-View VS Mono-View novel view synthesis.** Training both the original C3DGS as well as VIRGi using the proposed multi-view approach enhances the novel view synthesis results. We underline that VIRGi also provides a decomposition of the image into diffuse and specular.

metrics employed are standard radiance field metrics (PSNR, SSIM, and LPIPS), and the split between training and testing, as well as the recoloring editions, follows the protocol established in [15]. Importantly, VIRGi demonstrates a notable and consistent improvement over other radiance field recoloring methods, underscoring its efficacy and robustness.

Method robustness. The dataset provided by [15] contains 11 distinct recolored images for each scene in the MipNeRF-360 and LLFF datasets. To demonstrate the robustness of our approach to variations in the input image, we conducted 11 evaluations for each scene, each time using a different recolored ground-truth image as input. This methodology allows us to assess that the quality of our method remains consistent regardless of the specific input image chosen by the user for editing. The average recoloring PSNR for 11 iterations when modifying the edited image for VIRGi was (MipNeRF-360: 29.27, LLFF: 28.87), while for VANILLA-VIRGi it was (MipNeRF-360: 28.71, LLFF: 27.91). Remarkably, the average performance in both cases closely aligns with the standard experiment in Table I, using the images defined by [15] as the input image.

Ablation study. We analyze the individual contribution of each component with two ablation experiments. The first experiment (Table II), analyzes the impact of the decoupled output (DC), the multi-view rasterization (MV), and the integration of diffuse neuron activation into the segmentation network (DS). Notably, our method VIRGi emerges as the best-performing recoloring method overall. Adding multi-view information (MV) consistently enhances performance across all configurations. Moreover, the decoupled architecture (DC) demonstrates superior results with the utilization of multi-view. Remarkably, when multi-view is employed, the decoupled results consistently outperform the original non-decoupled color estimation. Additionally, inputting the diffuse neuron activations to the segmentation (DS) boosts performance in all cases except for a singular instance in the LLFF dataset. This outcome is reasonable, as the LLFF dataset comprises frontal recordings with limited viewpoint

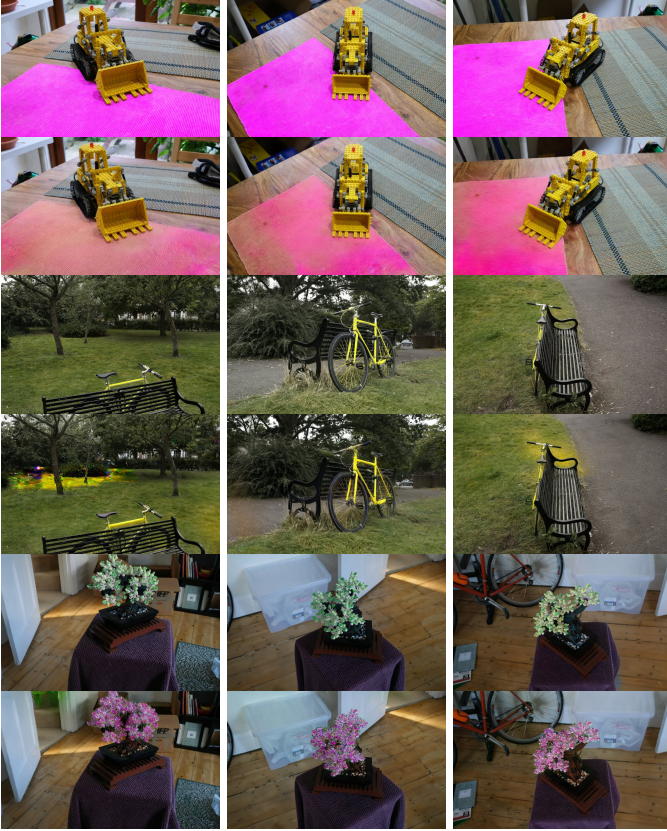


Fig. 5: Comparison between **VIRGi** (upper row per case) and **Gaussian Editor** [68] (bottom row per case). Gaussian Editor requires the user to initialize a mask using SAM [76] before applying color edits based on provided prompts: “kitchen - make it magenta”, “bicycle - make it yellow”, and “bonsai - make it green”. Gaussian Editor exhibits several drawbacks, such as color bleeding into surrounding areas in the first two scenes and not understanding the scene structure when recoloring the third scene. Notably, Gaussian Editor takes an average of 612 seconds to process these scenes, while **VIRGi** completes the task in just 2 seconds on average.

changes, thereby posing challenges in understanding diffuse and specular aspects of the scene.

In our second ablation experiment (Table III), we demonstrate how multiview optimization not only enhances the quality of the recoloring but also inherently improves the modeling of view-dependent effects in 3DGS. Specifically, we compare the reconstruction accuracy (without recoloring) of the original C3DGS [45] trained with and without multiview, and apply the same procedure to evaluate **VIRGi**. Notably, multiview consistently yields performance improvements across all cases. Furthermore, this experiment confirms that the proposed modifications to C3DGS [45] for color editing do not lead to any noticeable reduction in the original quality.

B. Qualitative results

Fig. 7 showcases qualitative results obtained from the MipNeRF-360 dataset [71]. This dataset features complex real scenes with complete 360° coverage. The edits produced by **VIRGi** demonstrate consistency across viewpoints and



Fig. 6: **Illumination editing with decoupled output**. Top row: specular component reduced by applying a multiplicative factor of 0. Bottom row: specular component increased by applying a factor of 1.5.

effectively capture the intricate view-dependent effects present in the scenes. Additionally, the 3D segmentation masks for each recolored region, estimated by our method, are presented, further illustrating its capability to achieve 3D consistency.

Comparison with Gaussian Editor. As discussed in Sect. II, no other method specifically addresses the challenge of performing appearance edition on Gaussian Splatting. However, some methods enable the modification of the final color of specific elements using text prompts. Fig. 5 presents a qualitative comparison of **VIRGi** and GaussianEditor [68]. GaussianEditor facilitates single-element recoloring by leveraging SAM [76] to generate a mask of the desired object. Subsequently, guided by a text prompt and employing Instruct-Pix2Pix [77], the scene edit is optimized until satisfactory results are achieved. As shown, our method is more consistently more robust. Notably, GaussianEditor exhibits color bleeding into undesired areas of the scene, a limitation not observed in **VIRGi**’s results. Additionally, while GaussianEditor requires approximately 10 minutes to complete a given edit, our approach achieves the same task in just 2 seconds, significantly enhancing its interactivity and usability.

Specular editing. In Fig. 6, we illustrate how decoupling the color output into diffuse and specular components enables fine adjustments to view-dependent effects. By manipulating the strength of the specular component C_{spec} , we can make subtle changes in the material appearance. Although the range of editions is limited, this experiment provides valuable insights into our model’s understanding of scene appearance, a key aspect of its superiority over other recoloring methods.

C. Limitations

While our approach excels in handling a wide range of color editing tasks, it has several limitations. First, our current material model with diffuse/specular separation is very simple, thus, more complex materials with transparency, anisotropy, or with colored reflections are not captured by the proposed representation. In Fig. 9, first and second rows, we show two examples of our decomposition. In the scene named as *Kitchen* (first row, the one with the Lego), the result appears more coherent and smooth, successfully separating reflections from the table and the top of the tractor wheels. While the *Kitchen*

scene handles reflections reasonably well, we observe that the decomposition breaks down in more complex cases, such as the mirror-like surfaces in the *Counter* scene (second row). As discussed previously, the goal of our decomposition is not physical accuracy but editability: specifically, enabling stable and multiview-consistent recoloring without degrading the final render. This is precisely why we introduced the separation of MLPs in our design: to ensure that recoloring operations target only the components unaffected by view direction, maintaining consistency across novel views. To show what our method would yield as a result in such failure cases, we have performed in Fig 9 some examples where we try to edit a transparent object, the water filter jug, and an object with a mirror-like surface, the bowl. In both cases our approach edits parts of the scene that it should not modify, generating a bleeding out of the color edit into other objects. Another limitation is that in certain cases a single edited view does not have enough information to segment the scene perfectly. This happens mainly in cases in which some parts of the scene, that were not present in the original edited image, are fairly similar to parts of the desired edition. Luckily, due to our method being interactive this can be easily fixed by adding a second edited image, as we show in the supplementary video. We show examples of wrong recoloring cases in Fig. 10. In those cases we show how we tried to solve the issues by adding a second edited image.

VI. CONCLUSIONS

We have presented a novel method that, by disentangling the color components and integrating multiview information during training, achieves high-quality in color editing for 3DGS. This represents a significant advancement, marking the first instance of a Gaussian splatting editing technique capable of generating recolored models of superior quality. Moreover, our method operates with remarkable speed (~ 2 seconds), rendering it highly suitable for interactive use by virtual production engineers or game designers seeking to efficiently edit assets. As future work, we aim to explore more complex materials and appearances, such as extending to specular color editing. Furthermore, investigating the minimum number of views required to ensure consistent representations while reducing memory consumption for complex edits is another promising direction.

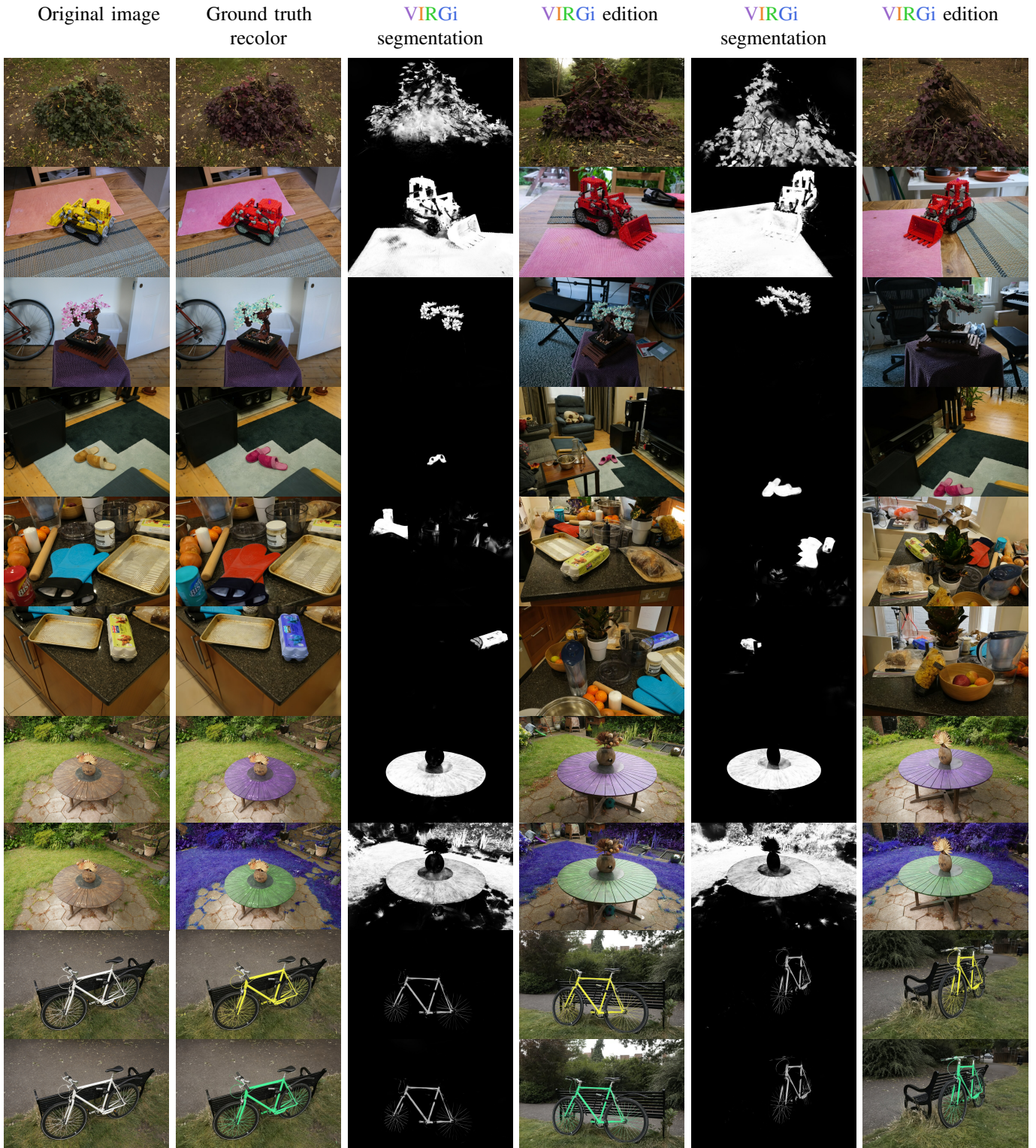


Fig. 7: **Qualitative results.** Results on all scenes from the MipNeRF-360 dataset [71]. This dataset shows complex real scenes with a complete 360 rotation on all scenes. We show several examples of single and multiple color editions. The first column is the original image. The second column is the edit performed by the user and used to train VIRGi. We also show the soft segmentation predicted by VIRGi for each recolored image.

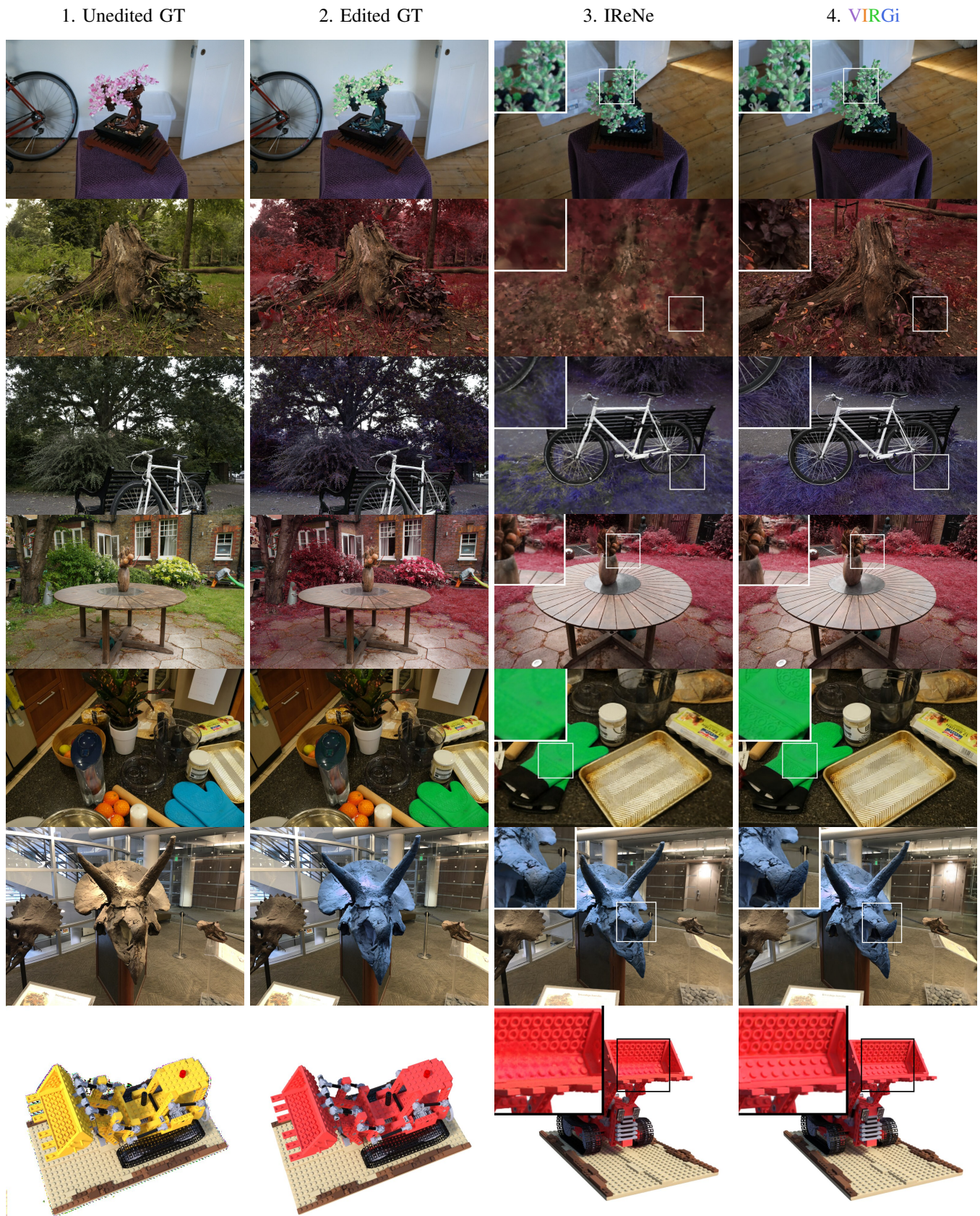


Fig. 8: Some qualitative results of the IReNe [15] dataset.

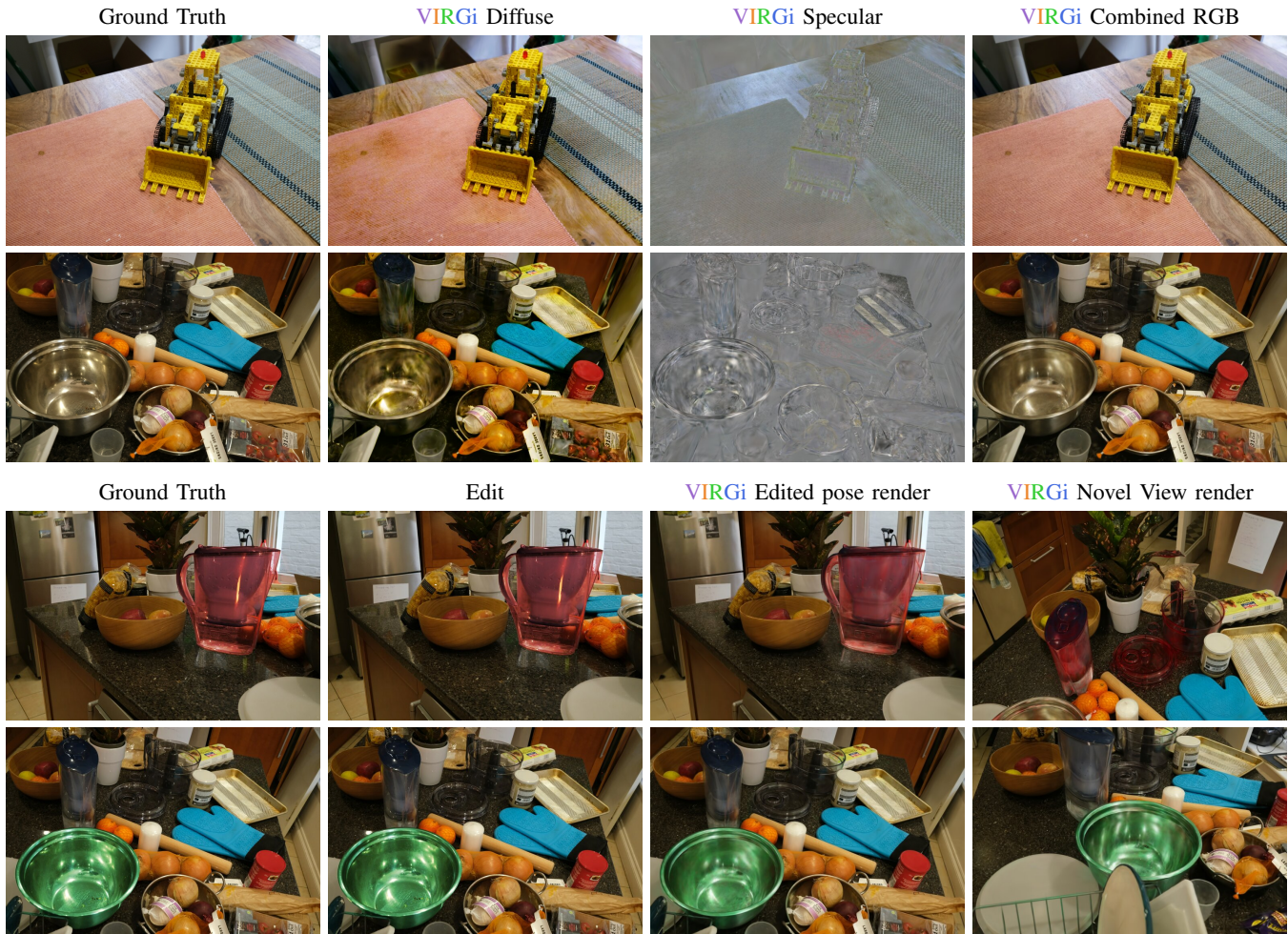


Fig. 9: **Limitations of diffuse/specular modeling.** First row **Kitchen** scene, second row **Counter** scene. Comparison between Ground Truth, Diffuse, Specular and Combined RGB render. Our simple diffuse/specular model struggles with complex or anisotropic materials. This can be seen in the Counter (bottom) scene, while the Kitchen (top) scene, especially the table, shows better results. Still, both yield solid RGB reconstructions. Third row - Fourth Row: Comparison of original, edited, and rendered views on specular failure cases. In the case of the water jug, although we are able to apply the recoloring, the result lacks uniformity: some areas of the jug appear more red than others, and the color bleeds onto objects visible through the jug's transparent surface. For the reflective bowl, we manage to change its color as well, but the edits are less clean compared to those on non-reflective, opaque objects. Some regions of the bowl retain the original color, with only a slight green tint appearing in the edited output



Fig. 10: **Limitations in segmentation.** We show examples where issues in recoloring happened. These cases occur mainly with parts of the scene that were not present in the first edited image. In the first example, the notebook has been incorrectly recolored. In the second example, the palm tree has been incorrectly recolored. In the third example, the legs of the table have not been fully recolored to red. These cases were fixed by adding a second edited image. In most cases, such issues can be solved by adding an additional edited image, but in some cases, like the last example, certain edits cannot be achieved. In this particular case, the curtain is far from the camera, and not much viewpoint change is present in the dataset from which to learn the correct model.



Alessio Mazzucchelli received the B.S. degree and the M.S. degree in computer engineering at Politecnico di Milano. He is currently pursuing the Ph.D. degree at Universitat Politècnica de Catalunya while developing its research at Arquimea Research Center. His research is mainly focused on editing implicit and explicit 3d representation.



Ivan Ojeda-Martin received the B.S. degree in computer engineering at Universidad de Las Palmas de Gran Canaria. He is currently developing research at Arquimea Research Center.



Fernando Rivas-Manzanaque received the B.S. degree and the M.S. degree in electrical engineering at Carlos III University of Madrid. He is currently pursuing the Ph.D. degree with Technical University of Madrid while developing its research at Volinga AI. His research is mainly focused on neural fields and his research interests include neural rendering, scene reconstruction, and image processing.



Elena Garces is a Senior Research Scientist at Adobe Paris since June 2024. Before that, she was Juan de la Cierva Fellow at the MSLab of the URJC and a Director at SEDDI (Madrid) where she led a technology area with expertise in render, optical capture, and AI. During 2016-2018, she was a Post-doctoral researcher at Technicolor R&D (France). She completed her Ph.D. in 2016 in the Graphics and Imaging Lab of the University of Zaragoza (Spain). During her Ph.D. she had the opportunity to intern twice at Adobe Research (San Jose and Seattle,

US). She proudly received the 2017 Premio de Investigación de la Sociedad Científica Informática de España y Fundación BBVA. Press coverage: FBBVA, Innova Spain, El País, El Mundo El Español. Her research interests span the fields of computer graphics, computer vision, and applied machine learning. In particular, I currently work on digitization (optics&physics) of fabric materials, machine learning-based simulations of garments, and 3D scene reconstruction.



Adrián Penate-Sanchez (PhD) received his PhD from the CSIC-UPC robotics lab (Institut de Robòtica i Informàtica Industrial) in Barcelona under the supervision of Juan Andrade Cetto and Francesc Moreno Noguier. In 2014, he joined the Computer Vision group at Toshiba's Cambridge Research Laboratory for a 5 month internship. From Nov 2015 till February of 2018 he was a Post-doctoral Research Associate at University College London (UCL) working in the fields of 3D computer vision and machine learning. In March of 2018 he

joined the University of Oxford as a Postdoctoral Research Associate working to find solutions to robot navigation in unstructured environments like forests. In 2020 he joined the University of Las Palmas de Gran Canaria as a Distinguished Researcher and Lecturer under a Beatriz Galindo grant.



Francesc Moreno-Noguier is a Research Scientist of the Spanish National Research Council at the Institut de Robòtica i Informàtica Industrial. His research interests are in Computer Vision and Machine Learning, with topics including human shape and motion estimation, 3D reconstruction of rigid and nonrigid objects and camera calibration. He received the Polytechnic University of Catalonia's Doctoral Dissertation Extraordinary Award, several best paper awards (e.g. ECCV 2018 Honorable mention, ICCV 2017 workshop in Fashion, Intl. Conf. on Machine Vision applications 2016), outstanding reviewer awards at ECCV 2012 and CVPR 2014, 2021, and Google and Amazon Faculty Research Awards in 2017 and 2019, respectively. He has (co)authored over 150 publications in refereed journals and conferences (including 10 IEEE Transactions on PAMI, 5 Intl. Journal of Computer Vision, 28 CVPR, 11 ECCV and 9 ICCV)

REFERENCES

- [1] B. Kerbl, G. Kopanas, T. Leimkühler, and G. Drettakis, "3d gaussian splatting for real-time radiance field rendering," *ACM Transactions on Graphics (TOG)*, vol. 42, no. 4, July 2023. [Online]. Available: <https://repo-sam.inria.fr/fungraph/3d-gaussian-splatting/>
- [2] B. Mildenhall, P. P. Srinivasan, M. Tancik, J. T. Barron, R. Ramamoorthi, and R. Ng, "Nerf: Representing scenes as neural radiance fields for view synthesis," in *Proceedings of the European Conference on Computer Vision (ECCV)*, 2020.
- [3] Y. Wang, Q. Wu, G. Zhang, and D. Xu, "Gstream: Learning 3d geometry and feature consistent gaussian splatting for object removal," *arXiv preprint arXiv:2404.13679*, 2024.
- [4] A. Guédon and V. Lepetit, "Sugar: Surface-aligned gaussian splatting for efficient 3d mesh reconstruction and high-quality mesh rendering," in *Proceedings of the IEEE/CVF conference on computer vision and pattern recognition*, 2024, pp. 5354–5363.
- [5] S. Zhou, H. Chang, S. Jiang, Z. Fan, Z. Zhu, D. Xu, P. Chari, S. You, Z. Wang, and A. Kadambi, "Feature 3dgs: Supercharging 3d gaussian splatting to enable distilled feature fields," in *The IEEE Conference on Computer Vision and Pattern Recognition (CVPR)*, 2024.
- [6] J. Fang, J. Wang, X. Zhang, L. Xie, and Q. Tian, "Gaussianeditor: Editing 3d gaussians delicately with text instructions," in *The IEEE Conference on Computer Vision and Pattern Recognition (CVPR)*, 2024.
- [7] J. Wu, J.-W. Bian, X. Li, G. Wang, I. Reid, P. Torr, and V. Prisacariu, "GaussCtrl: Multi-View Consistent Text-Driven 3D Gaussian Splatting Editing," *ECCV*, 2024.
- [8] S. Shen, J. Xu, Y. Yuan, X. Yang, Q. Shen, and X. Wang, "Draggaussian: Enabling drag-style manipulation on 3d gaussian representation," *arXiv preprint arXiv:2405.05800*, 2024.
- [9] T. Xie, Z. Zong, Y. Qiu, X. Li, Y. Feng, Y. Yang, and C. Jiang, "Physgaussian: Physics-integrated 3d gaussians for generative dynamics," 2024.
- [10] K. Liu, F. Zhan, M. Xu, C. Theobalt, L. Shao, and S. Lu, "Stylegaussian: Instant 3d style transfer with gaussian splatting," *arXiv preprint arXiv:2403.07807*, 2024.
- [11] D. Zhang, Z. Chen, Y.-J. Yuan, F.-L. Zhang, Z. He, S. Shan, and L. Gao, "Stylizedgs: Controllable stylization for 3d gaussian splatting," *arXiv preprint arXiv:2404.05220*, 2024.
- [12] B. Gong, Y. Wang, X. Han, and Q. Dou, "Recolornerf: Layer decomposed radiance fields for efficient color editing of 3d scenes," *arXiv preprint arXiv:2301.07958*, 2023.
- [13] Z. Kuang, F. Luan, S. Bi, Z. Shu, G. Wetzstein, and K. Sunkavalli, "Palettenerf: Palette-based appearance editing of neural radiance fields," in *Proceedings of the IEEE/CVF Conference on Computer Vision and Pattern Recognition*, 2023, pp. 20 691–20 700.
- [14] J.-H. Lee and D.-S. Kim, "Ice-nerf: Interactive color editing of nerfs via decomposition-aware weight optimization," in *Proceedings of the IEEE/CVF International Conference on Computer Vision (ICCV)*, October 2023, pp. 3491–3501.
- [15] A. Mazzucchelli, A. Garcia-Garcia, E. Garces, F. Rivas-Manzanaque, F. Moreno-Noguier, and A. Penate-Sanchez, "Irene: Instant recoloring of neural radiance fields," in *Proceedings of the IEEE/CVF Conference on Computer Vision and Pattern Recognition (CVPR)*, June 2024.
- [16] B. Wang, N. S. Dutt, and N. J. Mitra, "Proteusnerf: Fast lightweight nerf editing using 3d-aware image context," *arXiv preprint arXiv:2310.09965*, 2023.
- [17] M. Gross and H. Pfister, *Point-based graphics*. Elsevier, 2011.

- [18] M. Zwicker, M. Pauly, O. Knoll, and M. Gross, "Pointshop 3d: An interactive system for point-based surface editing," *ACM Transactions on Graphics (TOG)*, vol. 21, no. 3, pp. 322–329, 2002.
- [19] Y. Ohtake, A. Belyaev, M. Alexa, G. Turk, and H.-P. Seidel, "Multi-level partition of unity implicits," in *Acm Siggraph 2005 Courses*, 2005, pp. 173–es.
- [20] S. M. Seitz, B. Curless, J. Diebel, D. Scharstein, and R. Szeliski, "A comparison and evaluation of multi-view stereo reconstruction algorithms," in *Proceedings of the IEEE/CVF Conference on Computer Vision and Pattern Recognition (CVPR)*, vol. 1. IEEE, 2006, pp. 519–528.
- [21] T. Thonat, E. Shechtman, S. Paris, and G. Drettakis, "Multi-view inpainting for image-based scene editing and rendering," in *2016 Fourth International Conference on 3D Vision (3DV)*. IEEE, 2016, pp. 351–359.
- [22] S.-H. Baek, I. Choi, and M. H. Kim, "Multiview image completion with space structure propagation," in *Proceedings of the IEEE/CVF Conference on Computer Vision and Pattern Recognition (CVPR)*, 2016, pp. 488–496.
- [23] N. Snavely, S. M. Seitz, and R. Szeliski, "Photo tourism: exploring photo collections in 3d," in *ACM siggraph 2006 papers*, 2006, pp. 835–846.
- [24] G. Chaurasia, S. Duchene, O. Sorkine-Hornung, and G. Drettakis, "Depth synthesis and local warps for plausible image-based navigation," *ACM transactions on graphics (TOG)*, vol. 32, no. 3, pp. 1–12, 2013.
- [25] Z. Yang, X. Gao, W. Zhou, S. Jiao, Y. Zhang, and X. Jin, "Deformable 3d gaussians for high-fidelity monocular dynamic scene reconstruction," in *The IEEE Conference on Computer Vision and Pattern Recognition (CVPR)*, 2024.
- [26] G. Wu, T. Yi, J. Fang, L. Xie, X. Zhang, W. Wei, W. Liu, Q. Tian, and W. Xinggang, "4d gaussian splatting for real-time dynamic scene rendering," in *The IEEE Conference on Computer Vision and Pattern Recognition (CVPR)*, 2024.
- [27] D. Das, C. Wewer, R. Yunus, E. Ilg, and J. E. Lenssen, "Neural parametric gaussians for monocular non-rigid object reconstruction," in *The IEEE Conference on Computer Vision and Pattern Recognition (CVPR)*, 2024.
- [28] Y. Lin, Z. Dai, S. Zhu, and Y. Yao, "Gaussian-flow: 4d reconstruction with dynamic 3d gaussian particle," in *The IEEE Conference on Computer Vision and Pattern Recognition (CVPR)*, 2024.
- [29] Z. Li, Z. Chen, Z. Li, and Y. Xu, "Spacetime gaussian feature splatting for real-time dynamic view synthesis," in *The IEEE Conference on Computer Vision and Pattern Recognition (CVPR)*, 2024.
- [30] J. Sun, H. Jiao, G. Li, Z. Zhang, L. Zhao, and W. Xing, "3dstream: On-the-fly training of 3d gaussians for efficient streaming of photo-realistic free-viewpoint videos," in *The IEEE Conference on Computer Vision and Pattern Recognition (CVPR)*, 2024.
- [31] Z. Li, Z. Zheng, L. Wang, and Y. Liu, "Animatable gaussians: Learning pose-dependent gaussian maps for high-fidelity human avatar modeling," in *Proceedings of the IEEE/CVF Conference on Computer Vision and Pattern Recognition (CVPR)*, 2024.
- [32] M. Kocabas, R. Chang, J. Gabriel, O. Tuzel, and A. Ranjan, "Hugs: Human gaussian splats," in *Proceedings of the IEEE/CVF Conference on Computer Vision and Pattern Recognition (CVPR)*, 2024.
- [33] R. Abdal, W. Yifan, Z. Shi, Y. Xu, R. Po, Z. Kuang, Q. Chen, D.-Y. Yeung, and G. Wetzstein, "Gaussian shell maps for efficient 3d human generation," in *Proceedings of the IEEE/CVF Conference on Computer Vision and Pattern Recognition (CVPR)*, 2024.
- [34] S. Zheng, B. Zhou, R. Shao, B. Liu, S. Zhang, L. Nie, and Y. Liu, "Gps-gaussian: Generalizable pixel-wise 3d gaussian splatting for real-time human novel view synthesis," in *Proceedings of the IEEE/CVF Conference on Computer Vision and Pattern Recognition (CVPR)*, 2024.
- [35] L. Hu, H. Zhang, Y. Zhang, B. Zhou, B. Liu, S. Zhang, and L. Nie, "Gaussianavatar: Towards realistic human avatar modeling from a single video via animatable 3d gaussians," in *IEEE/CVF Conference on Computer Vision and Pattern Recognition (CVPR)*, 2024.
- [36] J. Xiang, X. Gao, Y. Guo, and J. Zhang, "Flashavatar: High-fidelity head avatar with efficient gaussian embedding," in *The IEEE Conference on Computer Vision and Pattern Recognition (CVPR)*, 2024.
- [37] H. Pang, H. Zhu, A. Kortylewski, C. Theobalt, and M. Habermann, "Ash: Animatable gaussian splats for efficient and photoreal human rendering," in *The IEEE Conference on Computer Vision and Pattern Recognition (CVPR)*, 2024.
- [38] Z. Qian, S. Wang, M. Mihajlovic, A. Geiger, and S. Tang, "3dgs-avatar: Animatable avatars via deformable 3d gaussian splatting," in *The IEEE Conference on Computer Vision and Pattern Recognition (CVPR)*, 2024.
- [39] Y. Yuan, X. Li, Y. Huang, S. De Mello, K. Nagano, J. Kautz, and U. Iqbal, "Gavatar: Animatable 3d gaussian avatars with implicit mesh learning," in *The IEEE Conference on Computer Vision and Pattern Recognition (CVPR)*, 2024.
- [40] B. Kerbl, A. Meuleman, G. Kopanas, M. Wimmer, A. Lanvin, and G. Drettakis, "A hierarchical 3d gaussian representation for real-time rendering of very large datasets," *ACM Transactions on Graphics*, vol. 44, no. 3, 2024.
- [41] Z. Fan, K. Wang, K. Wen, Z. Zhu, D. Xu, and Z. Wang, "Lightgaussian: Unbounded 3d gaussian compression with 15x reduction and 200+ fps," 2023.
- [42] K. Navaneet, K. P. Meibodi, S. A. Koohpayegani, and H. Pirsiavash, "Compact3d: Compressing gaussian splat radiance field models with vector quantization," *arXiv preprint arXiv:2311.18159*, 2023.
- [43] W. Morgenstern, F. Barthel, A. Hilsman, and P. Eisert, "Compact 3d scene representation via self-organizing gaussian grids," 2023.
- [44] S. Niedermayr, J. Stumpfegger, and R. Westermann, "Compressed 3d gaussian splatting for accelerated novel view synthesis," in *Proceedings of the IEEE/CVF Conference on Computer Vision and Pattern Recognition (CVPR)*, 2024.
- [45] J. C. Lee, D. Rho, X. Sun, J. H. Ko, and E. Park, "Compact 3d gaussian representation for radiance field," in *Proceedings of the IEEE/CVF Conference on Computer Vision and Pattern Recognition (CVPR)*, June 2024.
- [46] D. Verbin, P. Hedman, B. Mildenhall, T. Zickler, J. T. Barron, and P. P. Srinivasan, "Ref-nerf: Structured view-dependent appearance for neural radiance fields," in *2022 IEEE/CVF Conference on Computer Vision and Pattern Recognition (CVPR)*. IEEE, 2022, pp. 5481–5490.
- [47] T. Wu, J.-M. Sun, Y.-K. Lai, and L. Gao, "De-nerf: Decoupled neural radiance fields for view-consistent appearance editing and high-frequency environmental relighting," in *ACM SIGGRAPH 2023 conference proceedings*, 2023, pp. 1–11.
- [48] J. Zhang, Y. Yao, S. Li, J. Liu, T. Fang, D. McKinnon, Y. Tsin, and L. Quan, "Neif++: Inter-reflectable light fields for geometry and material estimation," in *Proceedings of the IEEE/CVF International Conference on Computer Vision*, 2023, pp. 3601–3610.
- [49] H. Wu, Z. Hu, L. Li, Y. Zhang, C. Fan, and X. Yu, "Nefir: Inverse rendering for reflectance decomposition with near-field indirect illumination," in *Proceedings of the IEEE/CVF Conference on Computer Vision and Pattern Recognition*, 2023, pp. 4295–4304.
- [50] S. Wu, S. Basu, T. Brodermann, L. Van Gool, and C. Sakaridis, "Pbrnerf: Inverse rendering with physics-based neural fields," *arXiv preprint arXiv:2412.09680*, 2024.
- [51] Z. Liang, Q. Zhang, Y. Feng, Y. Shan, and K. Jia, "Gs-ir: 3d gaussian splatting for inverse rendering," in *Proceedings of the IEEE/CVF Conference on Computer Vision and Pattern Recognition*, 2024, pp. 21 644–21 653.
- [52] S. Lai, L. Huang, J. Guo, K. Cheng, B. Pan, X. Long, J. Lyu, C. Lv, and Y. Guo, "Glossygs: Inverse rendering of glossy objects with 3d gaussian splatting," *IEEE Transactions on Visualization and Computer Graphics*, 2025.
- [53] Y. Shi, Y. Wu, C. Wu, X. Liu, C. Zhao, H. Feng, J. Zhang, B. Zhou, E. Ding, and J. Wang, "Gir: 3d gaussian inverse rendering for relightable scene factorization," *arXiv preprint arXiv:2312.05133*, 2023.
- [54] K. Ye, Q. Hou, and K. Zhou, "3d gaussian splatting with deferred reflection," in *ACM SIGGRAPH 2024 Conference Papers*, 2024, pp. 1–10.
- [55] Y. Endo, S. Iizuka, Y. Kanamori, and J. Mitani, "Deepprop: Extracting deep features from a single image for edit propagation," in *Computer Graphics Forum*, vol. 35, no. 2. Wiley Online Library, 2016, pp. 189–201.
- [56] X. An and F. Pellacini, "Approp: all-pairs appearance-space edit propagation," *ACM Transactions on Graphics (TOG)*, vol. 27, no. 3, pp. 1–9, 2008.
- [57] X. Chen, D. Zou, Q. Zhao, and P. Tan, "Manifold preserving edit propagation," *ACM Transactions on Graphics (TOG)*, vol. 31, no. 6, pp. 1–7, 2012.
- [58] "Scribbleboost: Adding classification to edge-aware interpolation of local image and video adjustments," in *Computer Graphics Forum*, vol. 27, no. 4. Wiley Online Library, 2008, pp. 1255–1264.
- [59] S. Meyer, V. Cornillère, A. Djelouah, C. Schroers, and M. Gross, "Deep video color propagation," in *Proceedings of the British Machine Vision Conference (BMVC)*, Newcastle upon Tyne, UK, September 3-6, 2018. British Machine Vision Association (BMVA), 2018.
- [60] B. Zhang, M. He, J. Liao, P. V. Sander, L. Yuan, A. Bermak, and D. Chen, "Deep exemplar-based video colorization," in *Proceedings of the IEEE/CVF Conference on Computer Vision and Pattern Recognition (CVPR)*, 2019, pp. 8052–8061.

- [61] H. Chang, O. Fried, Y. Liu, S. DiVerdi, and A. Finkelstein, "Palette-based photo recoloring," *ACM Transactions on Graphics (TOG)*, vol. 34, no. 4, pp. 1–11, 2015.
- [62] J. Tan, J. Echevarria, and Y. Gingold, "Efficient palette-based decomposition and recoloring of images via rgbxy-space geometry," *ACM Transactions on Graphics (TOG)*, vol. 37, no. 6, pp. 1–10, 2018.
- [63] Z.-J. Du, K.-X. Lei, K. Xu, J. Tan, and Y. Gingold, "Video recoloring via spatial-temporal geometric palettes," *ACM Transactions on Graphics (TOG)*, vol. 40, no. 4, Aug. 2021.
- [64] Z. Chen, F. Wang, and H. Liu, "Text-to-3d using gaussian splatting," in *The IEEE Conference on Computer Vision and Pattern Recognition (CVPR)*, 2024.
- [65] Y. Liang, X. Yang, J. Lin, H. Li, X. Xu, and Y. Chen, "Luciddreamer: Towards high-fidelity text-to-3d generation via interval score matching," in *The IEEE Conference on Computer Vision and Pattern Recognition (CVPR)*, 2024.
- [66] H. Ling, S. W. Kim, A. Torralba, S. Fidler, and K. Kreis, "Align your gaussians: Text-to-4d with dynamic 3d gaussians and composed diffusion models," in *The IEEE Conference on Computer Vision and Pattern Recognition (CVPR)*, 2024.
- [67] Y.-H. Huang, Y.-T. Sun, Z. Yang, X. Lyu, Y.-P. Cao, and X. Qi, "Sc-gs: Sparse-controlled gaussian splatting for editable dynamic scenes," in *The IEEE Conference on Computer Vision and Pattern Recognition (CVPR)*, 2024.
- [68] Y. Chen, Z. Chen, C. Zhang, F. Wang, X. Yang, Y. Wang, Z. Cai, L. Yang, H. Liu, and G. Lin, "Gaussianeditor: Swift and controllable 3d editing with gaussian splatting," in *Proceedings of the IEEE/CVF Conference on Computer Vision and Pattern Recognition (CVPR)*, 2024.
- [69] H. Yu, J. Julin, Z. A. Milacski, K. Niinuma, and L. A. Jeni, "Cogs: Controllable gaussian splatting," in *Proceedings of the IEEE/CVF Conference on Computer Vision and Pattern Recognition (CVPR)*, 2024.
- [70] M. Zwicker, H. Pfister, J. Baar, and M. Gross, "Surface splatting," *Proceedings of the ACM SIGGRAPH Conference on Computer Graphics*, vol. 2001, 08 2001.
- [71] J. T. Barron, B. Mildenhall, D. Verbin, P. P. Srinivasan, and P. Hedman, "Mip-nerf 360: Unbounded anti-aliased neural radiance fields," in *Proceedings of the IEEE/CVF Conference on Computer Vision and Pattern Recognition (CVPR)*, June 2022, pp. 5470–5479.
- [72] S. A. Shafer, "Using color to separate reflection components," *Color Research & Application*, vol. 10, no. 4, pp. 210–218, 1985.
- [73] S. Beigpour and J. Van De Weijer, "Object recoloring based on intrinsic image estimation," in *Proceedings of the IEEE/CVF Conference on Computer Vision and Pattern Recognition (CVPR)*. IEEE, 2011, pp. 327–334.
- [74] M. Pharr, W. Jakob, and G. Humphreys, *Physically based rendering: From theory to implementation*. MIT Press, 2023.
- [75] B. Mildenhall, P. P. Srinivasan, R. Ortiz-Cayon, N. K. Kalantari, R. Ramamoorthi, R. Ng, and A. Kar, "Local light field fusion: Practical view synthesis with prescriptive sampling guidelines," *ACM Transactions on Graphics (TOG)*, 2019.
- [76] A. Kirillov, E. Mintun, N. Ravi, H. Mao, C. Rolland, L. Gustafson, T. Xiao, S. Whitehead, A. C. Berg, W.-Y. Lo, P. Dollár, and R. B. Girshick, "Segment anything," *2023 IEEE/CVF International Conference on Computer Vision (ICCV)*, pp. 3992–4003, 2023. [Online]. Available: <https://api.semanticscholar.org/CorpusID:257952310>
- [77] T. Brooks, A. Holynski, and A. A. Efros, "Instructpix2pix: Learning to follow image editing instructions," in *CVPR*, 2023.